Journal of Experimental Botany, Vol. 59, No. 9, pp. 2529–2543, 2008
doi:10.1093/jxb/ern119
This paper is available online free of all access charges (see http://jxb.oxfordjournals.org/open_access.html for further details)

Journal of Experimental Botany
www.jxb.oxfordjournals.org

RESEARCH PAPER

IAA stimulates pollen tube growth and mediates the modification of its wall composition and structure in *Torenia fournieri*

Juan-Zi Wu[1], Yi Lin[2], Xue-Lian Zhang[1], Dai-Wen Pang[2] and Jie Zhao[1,*]

[1] *Key Laboratory of the Ministry of Education for Plant Developmental Biology, College of Life Sciences, Wuhan University, Wuhan, 430072, China*

[2] *College of Chemistry and Molecular Sciences, and State Key Laboratory of Virology, Wuhan University, Wuhan 430072, China*

Received 24 January 2008; Revised 27 March 2008; Accepted 31 March 2008

Abstract

The effects of several hormones on pollen tube growth were compared in *Torenia fournieri* and it was found that IAA was the most effective, stimulating pollen tube growth and causing the shank part of pollen tubes to be slender and straighter. The role of IAA was investigated by studying the changes in ultrastructure and PM H^+-ATPase distribution in the pollen tubes and the modification of the tube wall. Using the fluorescent marker FM4-64, together with transmission electron microscopy, it was shown that secretory vesicles and mitochondria increased in IAA-treated tubes. Immunolocalization and fluorescence labelling, together with Fourier-transform infrared analysis, detected that IAA enhanced the level of PM H^+-ATPase and the synthesis of pectins, and reduced the cellulose density in pollen tubes. Importantly, to observe the orientation of cellulose microfibrils in pollen tubes *in situ*, atomic force microscopy was used to examine the 'intact' tube wall. Atomic force microscopy images showed that cellulose microfibrils were parallel to each other in the subapical region of IAA-treated tubes, but disorganized in control tubes. All results provided new insights into the functions of cellulose microfibrils in pollen tube growth and direction, and revealed that the IAA-induced changes of pollen tubes were attributed to the increase in secretory vesicles, mitochondria, and PM H^+-ATPase, and the modification of pectin and cellulose microfibrils in the tube wall.

Key words: AFM, cellulose microfibrils, FTIR, IAA, PM H^+-ATPase, pollen tube, secretory vesicles, *Torenia fournieri*.

Introduction

The pollen tube is a highly polarized, rapidly tip-growing cell which provides an ideal model system for understanding the regulatory mechanism involved in tip-growing (Hepler *et al*., 2001). The pivotal problem of pollen tube growth is control of its growth rate and direction, which depends on the processes of polarized delivery and secretion of membrane and cell wall materials at the tube apex (Parton *et al*., 2001). Indole-3-acetic acid (IAA) has very important roles in plant sexual reproduction: controlling the development of stamens, gynoecia, and ovary, promoting the maturation of egg cells, inducing the axial polarity and polar development of the embryo (Nemhauser *et al*., 2000; Mol *et al*., 2004; Aloni *et al*., 2006). Some researches also reported the increase of free IAA in the pistil after pollination and suggested that IAA probably promotes pollen tube growth in the pistils (Kovaleva and Zakharova, 2003; Aloni *et al*., 2006). A previous study also confirmed that free IAA was present throughout the style tissue and its content increased after pollination in *T. fournieri* L. (Wu *et al*., 2008). In an *in vitro* culture system, IAA stimulated *T. fournieri* pollen tubes to grow into a long, straight shape compared with a short, kinked control tube. The mechanisms by which IAA regulates pollen tube growth and shape are still poorly understood.

* To whom correspondence should be addressed. E-mail: jzhao@whu.edu.cn

Abbreviations: AFM, atomic force microscopy; CMFs, cellulose microfibrils; CW, calcofluor white; FTIR, Fourier-transform infrared microscopy; GA_3, gibberellin; IAA, indole-3-acetic acid; PMEs, pectin methylesterases; SVs, secretory vesicles; TEM, transmission electron microscopy; ZT, zeatin.

Plant PM H^+-ATPase is known as a 'master enzyme' which, using ATP as the energy source, pumps protons from the cytoplasm to the cell exterior, thus creating an electrochemical gradient across the plasma membrane (Rober-Kleber *et al*., 2003). Several studies have shown that PM H^+-ATPase is involved in auxin-mediated cell elongation (Frias *et al*., 1996; Rober-Kleber *et al*., 2003). Furthermore, PM H^+-ATPase was suggested to play a major role in pollen tube growth (Fricker *et al*., 1997; Pertl *et al*., 2001). However, little information about the role of PM H^+-ATPase in IAA-induced pollen tube growth has been reported.

The plant cell wall, especially the cellulose microfibrils (CMFs), is likely to be the main regulator of cell growth and orientation (Roudier *et al*., 2005). Although there have been many reports of multiple functions for the cell wall in pollen tube growth, such as controlling cell shape, resisting mechanical damage and the turgor pressure, and adhering to the transmitting tissue (Geitmann and Steer, 2006), the precise mechanism by which the cell wall controls the tube shape is still unclear. An attempt was made to investigate the role of the tube wall in IAA-induced pollen tube growth in *T. fournieri*. Pollen tubes are long tubular cells whose cell wall materials are different in composition and configuration along their longitudinal axes (Geitman and Parre, 2004). Most traditional chemical analyses of plant cell walls are destructive, since they require disintegration of plant tissue, and difficulties of sample isolation arise when small cell wall areas are of interest. The characteristics of the tube wall compelled the use of methods which analyse the cell wall *in situ*. Fourier-transform infrared microscopy (FTIR) and atomic force microscopy (AFM) offer this opportunity (Toole *et al*., 2004; Ding and Himmel, 2006). Reports on the pollen tube wall (Zhang *et al*., 2005; Sheng *et al*., 2006) showed that FTIR was a reliable and highly reproducible spectroscopic technique that could provide *in situ* information of cell wall components. AFM offers high-resolution imaging for biological surfaces, which has been used to observe the walls of some 'intact' cells, such as grapevine cells and maize parenchyma cells (Lesniewska *et al*., 2004; Ding and Himmel, 2006).

In the present study, the fluorescent dye FM4-64 and transmission electron microscopy (TEM) were used to detect secretory vesicles (SVs) and ultrastructural changes and immunofluorescent labelling was used to investigate the PM H^+-ATPase distribution changes and fluorescence labelling of wall components (pectins and cellulose) which, together with FTIR, analysed the distribution and content changes of wall materials in pollen tubes of *T. fournieri*. Furthermore, AFM was used to observe the morphology of the pollen tube surface and the arrangement of CMFs. All these studies attempted to reveal the potential mechanisms by which IAA regulates pollen tube growth.

Materials and methods

Plant materials

Torenia fournieri plants were grown in a greenhouse at Wuhan University. Pollen was taken fresh from dehisced anthers 2 d after flower opening.

Pollen tube growth

In a preliminary study it was found that 4 mg l^{-1} (22.8 μM) IAA, 2 mg l^{-1} zeatin (ZT) (9.1 μM), or 4 mg l^{-1} (11.5 μM) gibberellin (GA_3) could notably stimulate pollen tube growth of *T. fournieri in vitro*. In this study, the work was continued to investigate the effects of mixed hormones on pollen tube growth. IAA, ZT, and GA_3 were added alone at a concentration of 4, 2, and 4 mg l^{-1} to the basal medium, respectively. Mixed hormones in the medium were as follows: (i) 4 mg l^{-1} IAA/2 mg l^{-1} ZT; (ii) 4 mg l^{-1} IAA/4 mg l^{-1} GA_3; (iii) 4 mg l^{-1} GA_3/2 mg l^{-1} ZT; (iv) 4 mg l^{-1} IAA/4 mg l^{-1} GA_3/2 mg l^{-1} ZT. The medium described by Higashiyama *et al*. (1998) was modified to be the basal medium for growth of *T. fournieri* pollen tubes. The concentration of $Ca(NO_3)_2.4H_2O$ was reduced to 50 mg l^{-1}. The pH of the medium was not changed by the addition of hormones. In other experiments, pollen was cultured in fresh basal medium supplemented with 4 mg l^{-1} IAA or without (control test) at 25 °C in the dark. The length and the diameter of the shank part of pollen tubes were measured by celiang software (http://ninghan.cn) and the diameter was detected at 15 μm from the tube tip. Experiments were repeated at least three times with 27–70 replicates in each group each time.

FM 4-64 labelling

After culture for 2 h, pollen tubes were stained with 3 μM FM4-64 (Molecular Probes) for 12 min, and then washed three times with basal medium. The tubes were observed under a microscope (DMIRE2, Leica, Solms, Germany) using green light excitation. Experiments were repeated three times.

SVs observed by TEM

Pollen tubes cultured for 2 h were fixed with 2% glutaraldehyde in 10 mM PBS, pH 7.2 for 2 h, then embedded into 2% agar and fixed in fresh fixatives under vacuum for 3 h. The preparation of pollen tubes for TEM observation followed the methods described by Zhao *et al*. (2002). Ultrathin sections were cut with an ultramicrotome (Sorvall MT-6000) and stained with uranyl acetate/lead citrate. The TEM micrographs were taken at 75 kV with a JEM 100/II transmission electron microscope. In each treatment 10–12 pollen tubes were taken for sectioning.

Immunofluorescent labelling of PM H^+-ATPases in pollen tubes

To detect PM H^+-ATPases, pollen tubes cultured for 2 h were fixed with 2.5% formaldehyde freshly prepared from paraformaldehyde in 10 mM PBS, pH 7.2, with 5% sucrose for 2 h, rinsed three times with 10 mM PBS, and incubated with the anti-PM H^+-ATPase*s* antibodies (Maudoux *et al*., 2000) diluted at 1/100 in 10 mM PBS overnight at 4 °C. The anti-PM H^+-ATPase*s* antibodies were generously provided by Professor Marc Boutry (Université Catholique de Louvain-la-Neuve). After three washes in the same buffer, samples were incubated with the secondary antibody, anti-rabbit-IgG–FITC conjugate (Sigma) diluted at 1/100 with PBS buffer for 2 h at 25 °C in dark. After several washes, the samples were observed under a Leica DMIRE2 microscope using blue light excitation. In order to confirm PM H^+-ATPase is plasma membrane-associated, plasmolysis

was induced in pollen tubes with 0.3 M sorbitol treatment and immunofluorescent labelling was performed as mentioned above. The control tests were performed by omitting the primary or the secondary antibody. Experiments were repeated three times.

Immunofluorescent labelling of pectins

To detect pectins, pollen tubes cultured for 2 h were fixed with 2.5% formaldehyde freshly prepared from paraformaldehyde in 10 mM PBS, pH 7.2, with 5% sucrose for 2 h, rinsed three times with 10 mM PBS, and incubated with the primary monoclonal antibodies JIM5 (recognizing acid pectin) or JIM7 (recognizing esterified pectin) (diluted at 1/10) and the secondary antibody, anti-rat-IgG–FITC conjugate (Sigma) (diluted at 1/100). Monoclonal antibodies JIM5 and JIM7 were generously provided by Dr Paul Knox (University of Leeds, UK). Samples were observed under a confocal laser scanning microscope (TCS-SP, Germany). Excitation was at 488 nm, and fluorescence was detected at 510–560 nm. A 40× (0.75 NA) dry PL APO objective was used. All images were taken under the same conditions. The control tests were performed by omitting the primary or the secondary antibody. Experiments were repeated at least three times with 5–10 replicates in each group each time.

Detection of cellulose

To visualize cellulose, the fixed pollen tubes were incubated with 0.1% calcofluor white (CW) for 15 min. After three washes, samples were observed under a Leica DMIRE2 microscope using UV light excitation. To quantify the fluorescence, the captured images were first converted to 256 gray levels, then the entire tubes were traced and the total and average gray levels of pixels falling within the tubes were measured. Experiments were repeated three times with 9–15 replicates in each group each time.

FTIR analysis

After being cultured for 2 h, the pollen tubes were collected and washed three times with deionized water and then dried on a silver-gilt slide at room temperature. Infrared spectra were obtained from 20×20 μm areas in the apical region (clear zone) and sub-apical (~130–150 μm from the tube tip) region (organelle and nuclear zone) of the pollen tubes, respectively, under a Nicolet continuum FTIR microscope (Thermo Electron Corporation, USA) equipped with a mercury–cadmium–telluride detector. The spectra were recorded at a resolution of 8 cm^{-1} with 64 coadded interferegrams. The spectrum between 800 and 1800 cm^{-1}, which contains information of polysaccharides, was selected in order to monitor cell wall modifications. Assignments of the main bands in FTIR spectra were taken from these sources (Synytsya *et al*., 2003; Toole *et al*., 2004; Barron *et al*., 2005; Jones *et al*., 2005; Zhang *et al*., 2005; Sheng *et al*., 2006). Experiments were repeated at least three times with three or four replicates in each group each time.

AFM imaging

The hydrated pollen was placed on a cover slide previously coated with 0.1% (w/v) poly-L-lysine (Sigma, USA) to immobilize the pollen. After culture, fixation, and rinsing as described in the method of pectin labelling, the samples were washed four times with deionized water and lyophilized with a freeze dryer (Maxi Dry Lyo, Heto-Holten, USA). The AFM images were acquired in air (relative humidity = 50–60%, T=~20 °C) using the tapping mode of a NanoScope IV Extended MultiMode AFM (Digital Instruments, Inc., Santa Barbara, CA, USA) and a 'J' scanner. Commercially etched Si cantilevers (resonance frequency = ~300 kHz, spring constant = ~42 N m^{-1}) were used. All images were reproducible and rastered at 256×256 pixels. The software Nanoscope 5.12 was used for AFM operating and subsequent image processing. Experiments were repeated three times.

Results

Effects of various exogenous hormones on pollen tube growth

The effects of exogenous hormones on pollen tube growth were displayed in Fig. 1. When each hormone was used alone, IAA was the most effective hormone stimulating tube growth. IAA interacting with ZT and/or GA_3 stimulated tube growth much more than IAA used alone. However, the mix of ZT with GA_3 had no obvious effect on tube growth. In addition, the control tube had a rougher surface (Fig. 4A), compared with the IAA-treated tube which had a relatively smooth surface (Fig. 4B). Also the shank (in the region ~15 μm behind the tip) of the IAA-treated tubes was narrower and straighter (Table 1; Fig. 4B) than that of control tubes (Fig. 4A), but ZT and GA_3 had no effect on tube shape. These results suggest that IAA might be a primary hormonal promoter stimulating pollen tube growth.

FM4-64 staining

The FM4-64 labelling pattern was similar in control and IAA-treated tubes, i.e. the fluorescence staining focused in the tube apex and extended to the subapical region with a gradually lower intensity (Fig. 2A, C). However, the labelled region, which was deemed to be filled with SVs,

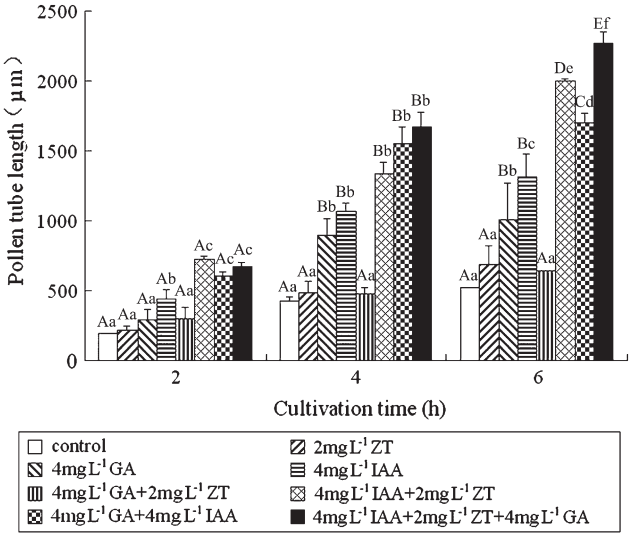

Fig. 1. Effects of IAA, ZT, and GA_3 on pollen tube growth in *Torenia fournieri*. Vertical bars represent standard errors in three independent experiments. Means denoted by the same upper-case letters and the same lower-case letters do not significantly differ at $P < 0.01$ and $P < 0.05$, respectively, according to the LSD (least significant difference) test. Comparison was made on the same treatment time.

Table 1. *Influence of IAA on the diameter of* in vitro *pollen tubes in* Torenia fournieri

Values given in the table are means and standard errors of three experiments. The analysis of significant variance was performed between the control group and IAA treatment according to Student's unpaired *t*-test. Comparison was made on the same treatment time.

Culture time (h)	Treatment	No. of pollen tubes	Diameter (μm)[a]
1	Control	210	11.61±1.83
	IAA	174	10.98±1.43**
2	Control	94	11.53±0.38
	IAA	82	8.07±0.03**
4	Control	115	8.83±0.25
	IAA	110	7.36±0.06**

[a]** $0.001 < P < 0.01$ indicates distinct difference.

was longer and the intensity of staining was stronger in IAA-treated tubes than in control tubes (Fig. 2).

Ultrastructure of pollen tubes observed by TEM

Pollen tubes have a marked polarity with four distinct zones along the tubes, i.e. clear zone, organelle zone, nuclear zone, and vacuolar zone (Cresti *et al*., 1985). TEM observation showed that the clear zone was abundant in SVs (Fig. 3A, B). SVs were evenly distributed in this zone of the control tubes, with an average density about 22/μm^2 (Fig. 3A). Both the middle sections and other deflective sections of pollen tube tip showed that more SVs (with an average density about 42/μm^2) and organelles, especially mitochondria, appeared in the clear zone after IAA treatment (Fig. 3B). In the organelle zone (10–150 μm from tube tip), more SVs and organelles, such as mitochondria, occurred in the IAA-treated tubes than in the control tubes (Fig. 3C, D). Also, in both the nuclear and the organelle zone, there were bigger vacuoles in IAA-treated tubes (Fig. 3E–H).

PM H$^+$-ATPase distribution in pollen tubes

After plasmolysis, the immunosignal of PM H$^+$-ATPase appeared in the plasma membrane, not in the cell wall of the pollen tubes (Fig. 4C, D). This enzyme was concentrated in the apical region of control tubes (Fig. 4E, F), while it was distributed throughout the tubes and was focused at the apical region after IAA treatment (Fig. 4G, I). IAA significantly increased the level of PM H$^+$-ATPases in pollen tubes (Fig. 4G–J). No labelling was observed in the absence of primary or secondary antibodies (pictures not shown).

Pectin distribution in pollen tubes

In mature pollen grains, the weak labelling of esterified pectin and acid pectin was present in all three germination apertures (Fig. 5A, H). When pollen grains had just germinated (after 0.5 h of culture), both pectins were mainly localized at the extruded tube tips (Fig. 5B, I). Esterified pectin was distributed along the entire tube after 1 h of culture (Fig. 5C, E) and concentrated at tube tips after 2 h of culture (Fig. 5D, F), while acid pectin was distributed throughout the whole tube at all times (Fig. 5J–N). Although the distribution pattern of pectins was similar in IAA-treated and control tubes, there was stronger labelling of both pectins in the former (Fig. 5C–F, J–N).

Cellulose distribution in pollen tubes

Cellulose fluorescent signals were distributed along the entire pollen tubes and increased towards the distal parts

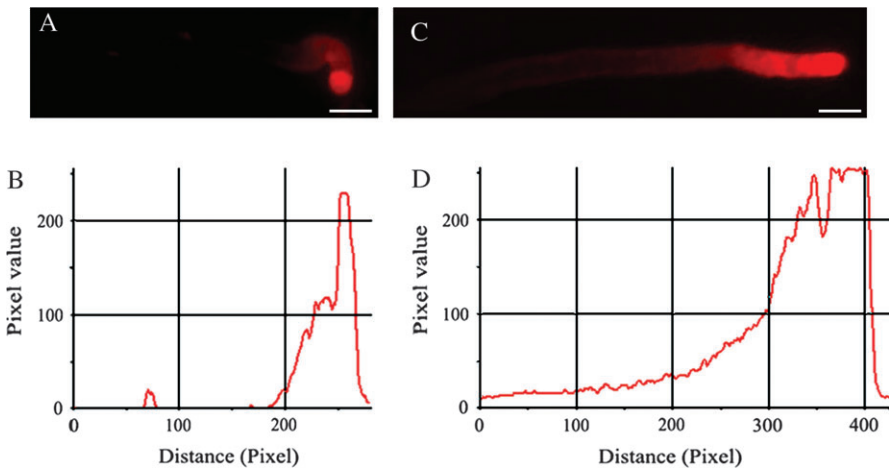

Fig. 2. The FM4-64 staining in pollen tubes of *Torenia fournieri*. (A, C) FM4-64 fluorescence images of pollen tubes cultured without and with IAA treatment for 2 h, respectively, showing the FM4-64 staining signal focused at the tube apex and extended to the subapical region with gradually lower intensity. (B, D) Pixel values along the longitudinal axes of the tubes in (A) and (C), respectively, showing the significant increase of fluorescence intensity in IAA-treated tubes. Bars = 15 μm (A), 12 μm (C).

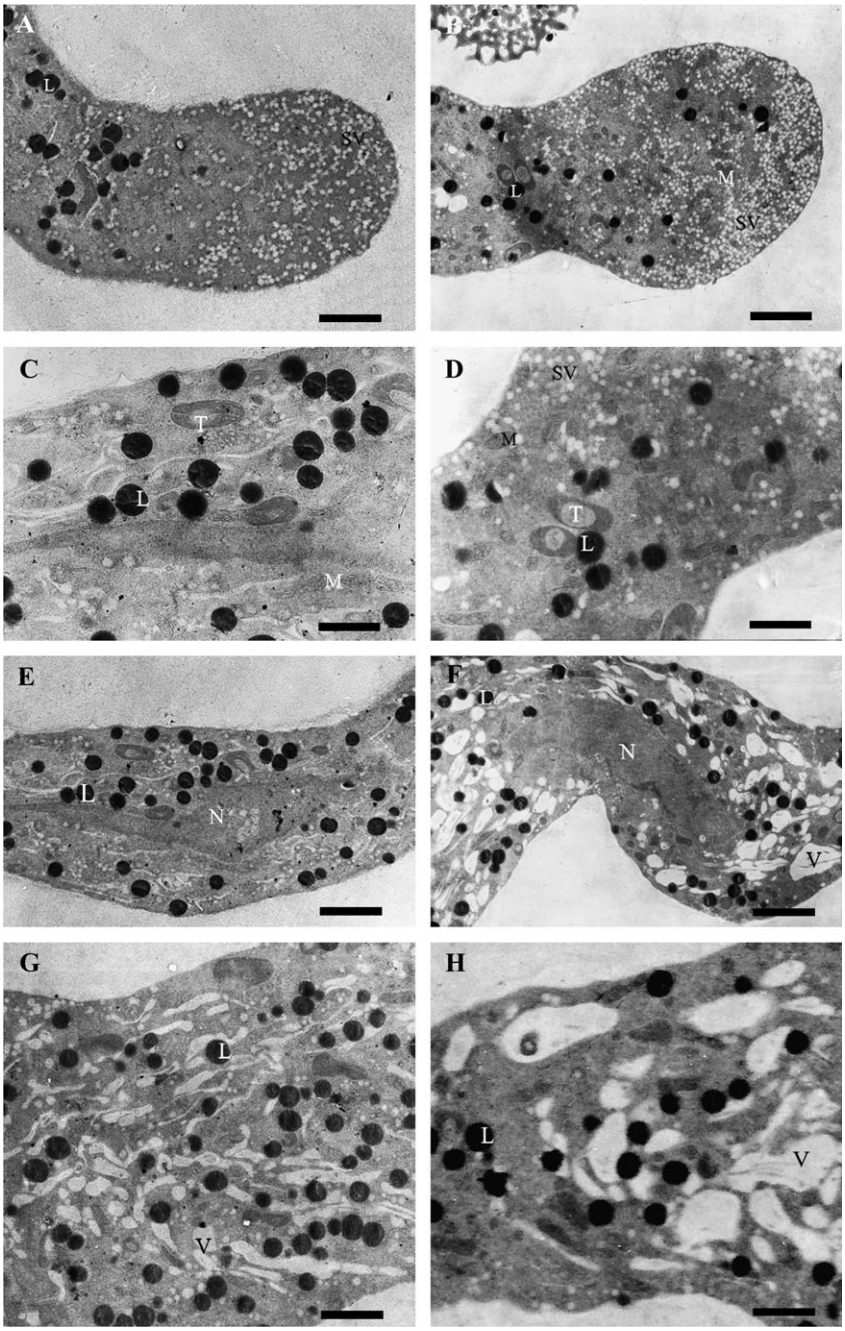

Fig. 3. TEM images of control (A, C, E, G) and IAA-treated (B, D, F, H) pollen tubes after 2 h of culture of *Torenia fournieri*. (A) The clear zone of a control tube, showing the vesicle-rich zone. (B) The clear zone of a treated tube, showing a dramatic increase in secretory vesicles (SVs) and appearance of organelles, e.g. mitochondria (M) in this zone. (C) The organelle zone of a control tube, showing some organelles, such as mitochondria, trophoplasts (T), and lipid bodies (L). (D) The organelle zone of a treated tube, showing more SVs and mitochondria. (E) The nuclear zone of a control tube, showing the spindly tube nucleus (N). (F) The nuclear zone of a treated tube, showing the spindly tube nucleus and abundant vacuoles (V). (G) Subapical region of a control tube filled with long strip-shaped and small round-shaped vacuoles. (H) Subapical region of a treated tube occupied by big vacuoles. Bars = 1.6 μm (A, G), 2 μm (B, F), 1 μm (C, D), 1.8 μm (E), 1.3 μm (H).

of tubes after 1 h of culture (Fig. 6A, D, E). More cellulose was present in the front part than the back part of the tubes after 2 h of culture (Fig. 6F–I). As tubes grew, the average cellulose fluorescence intensity significantly declined (Fig. 6A–C; Table 2). IAA lowered the average cellulose fluorescence intensity in tubes, especially in the apical region (Fig. 6B, C, F–I; Table 2), though the distribution pattern of cellulose was alike in IAA-treated and control tubes. The total cellulose fluorescence value of pixels falling within the tubes between control and IAA-treated tubes was not obviously different at all times (Table 2).

Changes in chemical components of the cell wall of pollen tubes

FTIR spectra were analysed in apical and subapical regions of pollen tubes, which showed similar patterns in these two regions. The absorption bands which occurred at 1626 and 1525 cm^{-1} corresponded to amide I and amide II of proteins, while the peaks at 1734 cm^{-1} were associated with esterified pectin and polysaccharides absorbed at 1200–900 cm^{-1} (Fig. 7A, B). A single principal component score that accounted for over 60.7% in the apical region (Fig. 7C) and 81.6% in the subapical region (Fig. 7D) of the total spectral variation could separate IAA-treated tubes from control tubes. IAA induced displacements of the peaks and changes in absorbance (Fig. 7A, B). The difference spectra generated by digital subtraction of control spectra from IAA-treated spectra showed that protein (peaks at 1653 and 1645 cm^{-1}, corresponding to amide I of proteins; 1552 and 1533 cm^{-1} corresponding to amide II of proteins) and pectin (peaks at 1745 cm^{-1}, corresponding to carboxylic ester in esterified pectin; 1263 cm^{-1}, corresponding to esterified pectin; 1105 cm^{-1}, corresponding to the backbone vibrations of polygalacturonic acid; 1024 cm^{-1}, corresponding to C-O stretching vibrations in pectin; 967 cm^{-1}, corresponding to pectate; 954 cm^{-1}, C-O bending vibration in pectin; 930 cm^{-1}, corresponding to pectin *O*-acetyl band) increased while cellulose (troughs at 1363, 1132, 1093, 1055, and 1024 cm^{-1}) decreased in tubes after IAA treatment (Fig. 7E, F).

Ultrastructure of pollen tubes observed by AFM

In AFM imaging, the AFM tip was positioned at the apical and sub-apical regions of the pollen tubes with the aid of a Nikon optical microscope and the scanned areas were gradually reduced (20, 5, 3, 2, and 1 μm^2). Also, the same areas of the control tubes and IAA-treated tubes were compared. To do this, the regions of the pollen tubes in focus were placed in the same direction as their longitudinal axes (Fig. 8). The images of the 'intact' tube walls obtained with the same probe showed that the tube surfaces were covered with block-like structures and/or fibrous structures (Fig. 8). The height and diameter of each structure, as well as the angle between the fibrous structure and the longitudinal axis, were measured (Table 3). The fibrous structures can be considered as CMFs according to their shapes and sizes, while the block-like structures were probably the outer tube wall matrix which was mainly composed of pectins. The arrangement of CMFs in the pollen tubes of *T. fournieri* was discerned in the phase images. The apical region of the control tube surface was rich in disorganized CMFs and block-like structures (Fig. 8A, B), while the IAA-treated tube surface was covered with both block-like structures approximately parallel to each other and a few CMFs (Fig. 8C, D). CMFs formed sinuous networks in the subapical region of control tube surface (Fig. 8E, F). However, numerous CMFs in the subapical region of IAA-treated tubes were parallel to each other and showed a predominant orientation at approximately $46.1 \pm 3.4°$ ($n=12$) to the longitudinal axes of the tubes (Fig. 8G, H). For IAA-treated tubes, the density of CMFs in the apical region was lower (Fig. 8D) than that in the subapical region (Fig. 8H).

Discussion

IAA stimulates pollen tube growth and changes tube shape

IAA promotes cell elongation in various plants, and the prevailing model of auxin for stimulating cell elongation is the 'acid-growth theory' which postulates that auxin increases the activity or amount of PM H^+-ATPase which triggers excretion of H^+ into the cell wall, and this acidification loosens the wall, allowing the cell to expand (Rayle and Cleland, 1992). Though some studies revealed that IAA affected pollen tube growth (Addicott, 1943; Raghavan and Baruah, 1956, 1959; Chauhan and Katiyar, 1998), the knowledge of its mechanism is still very limited. In the present study, IAA was the most effective hormone prompting tube growth (Fig. 1). Moreover, IAA led to a longer, straighter, and slender tube shape compared with the short, kinked control tubes (Fig. 4A, B). It seems reasonable to assume that IAA is one of the most important hormones regulating pollen tube growth.

IAA leads to an increase in the number of SVs and mitochondria in pollen tubes

The elongation of the pollen tube is determined by the continuous transportation and fusion of SVs in the tip region, which provide abundant new membrane and cell wall precursors for the growing pollen tube (Hepler *et al*., 2001; Parton *et al*., 2001). The fluorescent dye FM4-64 is an important tool in studying SVs and has been widely used as an authentic marker of vesicle accumulation in pollen tubes (Parton *et al*., 2001). The experiment with FM4-64 in *T. fournieri* pollen tubes revealed a longer labelled region and a stronger labelling intensity in IAA-treated tubes (Fig. 2), indicating that IAA increased the number of SVs in pollen tubes. This result was consistent with the observation that IAA treatment caused a substantial increase of SVs in pollen tubes in TEM images (Fig. 3A–D). It was also found that IAA enhanced the content of esterified pectin (Fig. 5) which was secreted into the tube cell wall by exocytosis. So it can be concluded that the quicker growth rate induced by IAA was largely caused by the promotion of the SVs and the stimulation of exocytosis in pollen tubes. Mitochondria are power centres of cells and provide ATP for cell

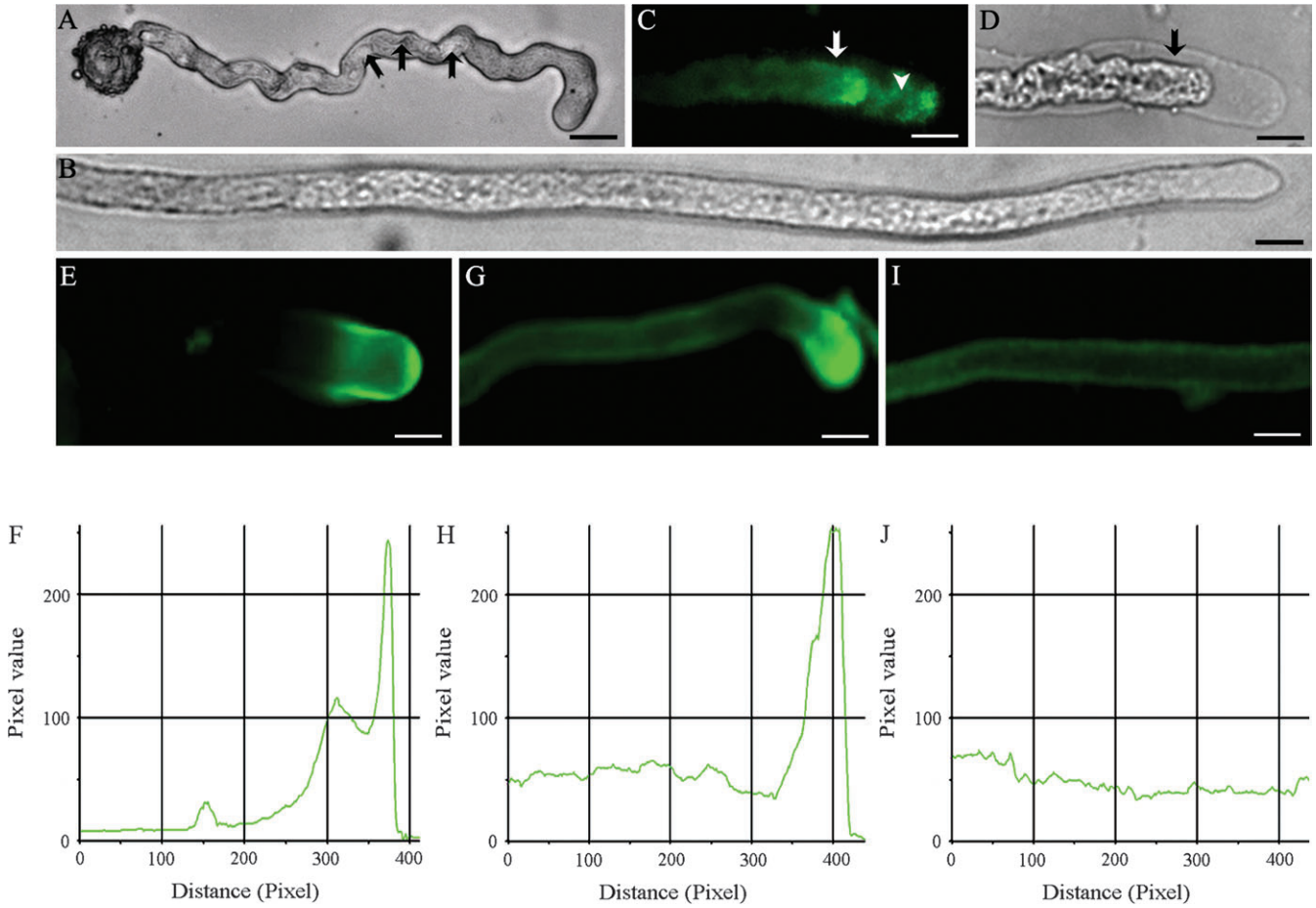

Fig. 4. Effects of IAA on *in vitro* pollen tube shape and immunofluorescent labelling of PM H^+-ATPase in *Torenia fournieri*. (A) A control pollen tube cultured for 2 h, showing the kinked, coiled shape. The arrows indicate the rough surface of the tube. (B) The forepart of an IAA-treated pollen tube cultured for 2 h, showing a smooth, straight shape. (C) The immunosignal of PM H^+-ATPase in a plasmolized pollen tube, showing fluorescence associated with the plasma membrane, not the cell wall (arrow). The arrowhead indicates the fluorescence associated with the unshed membranes at the apex. (D) Corresponding bright field image of (C). (E, G) Immunofluorescent images of PM H^+-ATPase in control (E) and IAA-treated (G) tubes. (I) Immunofluorescent images of PM H^+-ATPase in the middle part of an IAA-treated tube, showing PM H^+-ATPase accumulates at the tube apex. (F, H, J) Pixel values along the central longitudinal axes of the tubes in (E), (G), and (I), respectively. Bars = 18 μm (A), 13 μm (B), 8 μm (C, D), 6 μm (E, G, I).

growth and division (Moller, 2001). In the present study, IAA treatment increased the number of mitochondria in the pollen tube (Fig. 3A–D). The results indicated that IAA stimulated the respiration and metabolism of the tubes.

PM H^+-ATPases are correlated with IAA-induced pollen tube growth

Though PM H^+-ATPases are important for pollen tube growth (Fricker *et al*., 1997; Pertl *et al*., 2001), information about the distribution of PM H^+-ATPases in pollen tubes is limited. In *Lilium longiflorum*, PM H^+-ATPases, detected with a monoclonal antibody, were abundant in pollen grains but not in pollen tubes (Obermeyer *et al*., 1992). In *Nicotiana plumbaginifolia*, PM H^+-ATPases accumulated in the middle region of the pollen tube (Lefebvre *et al*., 2005). In the present study, by using the same polyclonal antibody used in *N. plumbaginifolia*, PM H^+-ATPases showed a tip-accumulated pattern in the apical domain (Fig. 4E, G). The discrepancy of these three results might be caused by different antibodies or plant species used.

Feijo *et al*. (1999) reported that there was an acidic domain at the extreme apex and a constitutive alkaline band at the base of the clear zone, which was consistent with an H^+ influx at the extreme apex and a marked efflux in the alkaline band. So they presumed that PM H^+-ATPase would be present near the base of the clear zone and be involved in creating the pH_{cyt} gradient that is along the pollen tube and intimately associated with the tube growth. The results in *N. plumbaginifolia* seem to support this hypothesis. However, in the present study, the tip-focused PM H^+-ATPases in *T. fournieri* pollen tube might lead to extrusion of H^+ from the tube tip. The

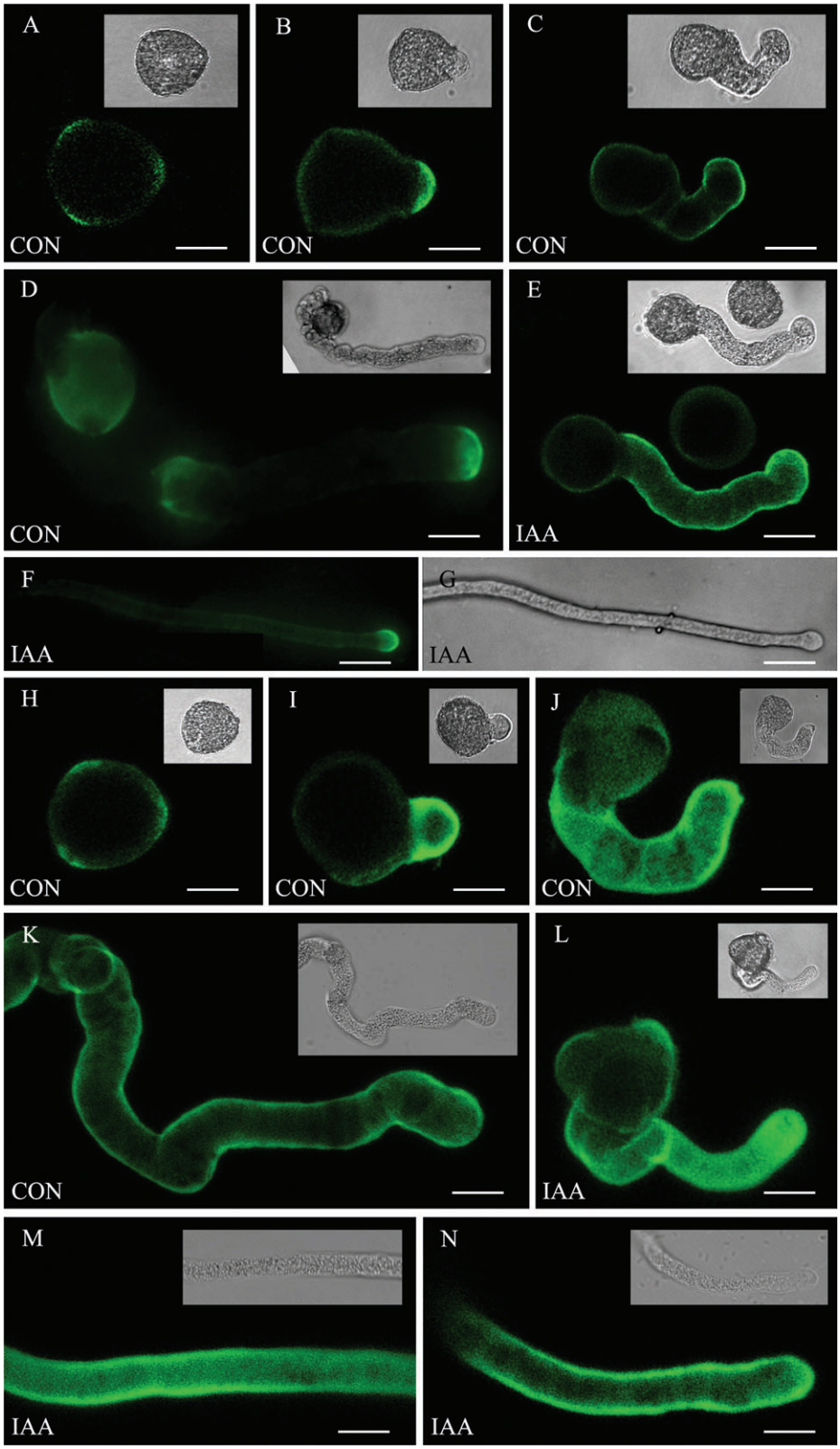

Fig. 5. Effects of IAA on the distribution of pectins in *Torenia fournieri* pollen tubes. Controls (A–D, H–K, CON) and IAA-treated (E–G, L–N, IAA) tubes were labelled with JIM7 (recognizing esterified pectin) (A–G) and JIM5 (recognizing acid pectin) (H–N). (A, H) Mature pollen grains. (B, I) Control tubes cultured for 30 min. (C, J) Control tubes cultured for 1 h. (D, K) Control tubes cultured for 2 h. (E, L) IAA-treated tubes cultured for 1 h. (F, N) The forepart of an IAA-treated tube cultured for 2 h. (G) Corresponding bright field image of (F). (M) The middle part of an IAA-treated tube cultured for 2 h. The inset pictures are the corresponding bright field images. Bars = 15 μm (A, B, D, H–J, L–N), 22 μm (C, E), 67 μm (F, G), 17 μm (K).

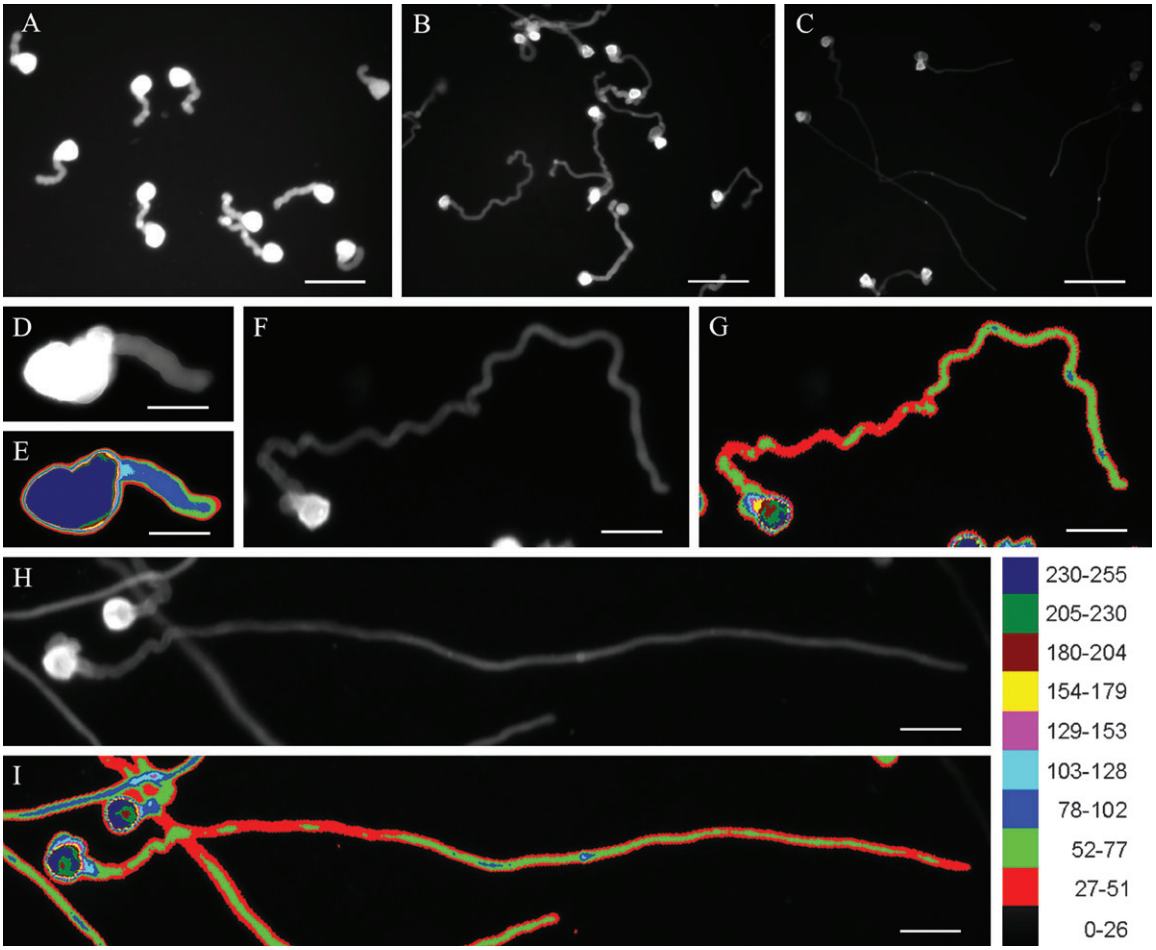

Fig. 6. Effects of IAA on the distribution of cellulose in *Torenia fournieri* pollen tubes cultured for 1 h (A, D, E) and 2 h (B, C, F–I). Controls (A, B, D–G) and IAA-treated (C, H, I) tubes were labelled with calcofluor white. (A–D, F, H) Cellulose fluorescence images of pollen tubes. (E, G, I) Pseudocolour images of pollen tubes corresponding to (D), (F), and (H), respectively. The colour scale referred to cellulose fluorescence intensities. Bars = 95 μm (A), 146 μm (B), 182 μm (C), 39 μm (D, E), 53 μm (F–I).

Table 2. *Influence of IAA on the cellulose density of* in vitro *pollen tubes in* Torenia fournieri

Values given in the table are means and standard errors of three experiments. The analysis of significant variance was performed between the control group and IAA treatment according to Student's unpaired *t*test. Comparison was made on the same treatment time.

Culture time (h)	Treatment	No. of pollen tubes	The average fluorescence value	The total areas of pixels falling within pollen tubes	The total cellulose fluorescence value of pixels falling within pollen tubes
0.5	Control	26	138±5	573±45	79030±3545
	IAA	45	106±4***	742±90**	75569±5186*
1	Control	44	94±9	1039±313	114882±258
	IAA	35	86±5**	1036±211*	99927±2524*
2	Control	38	67±3	10757±2760	175715±94
	IAA	37	48±4***	12402±3913**	181772±27*

* $P > 0.05$ indicates no difference; ** $0.01 < P < 0.05$ indicates distinct difference; *** $P < 0.01$ indicates extreme distinct difference.

possible explanation is that PM H^+-ATPases followed the secretory pathway to reach the tube apex and through Ca^{2+}-dependent phosphorylation, high $[Ca^{2+}]_i$ at the tube apex would inhibit the activity of the PM H^+-ATPases (Feijo *et al*., 1999). When moving with cytoplasmic streaming back from the tip where the $[Ca^{2+}]_i$ is at a lower level, this enzyme would trigger excretion of H^+ into the cell wall. As a matter of fact, evidence that pH_{cyt} gradients in pollen tube are involved in regulating tube growth remain controversial (Fricker *et al*., 1997; Parton *et al*.,

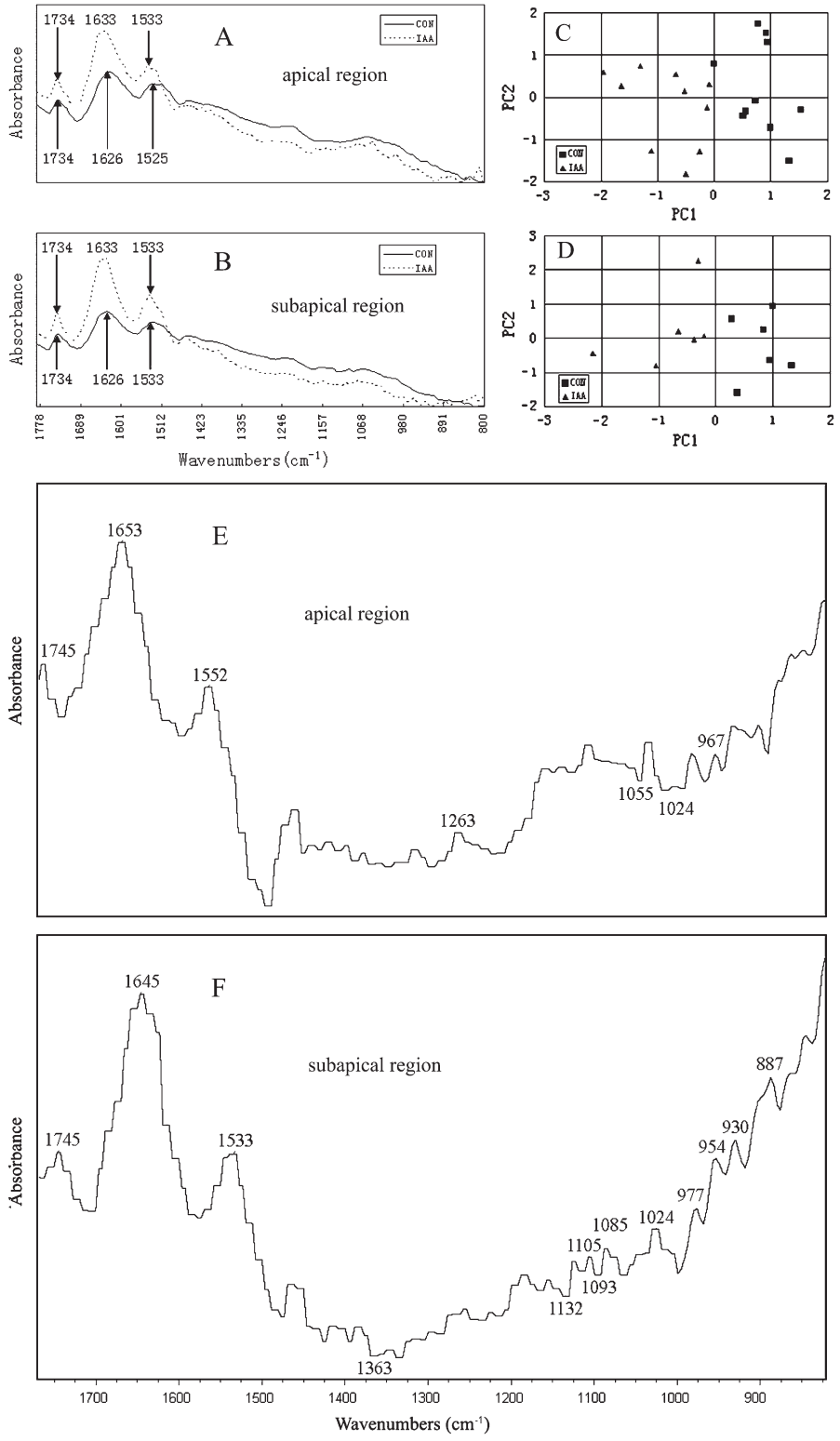

Fig. 7. Analysis of FTIR spectra from pollen tubes of *Torenia fournieri*. (A, B) Average FTIR spectra obtained from the apical region (n=10) (A) and subapical region (n=6) (B) of pollen tubes cultured for 2 h under control conditions (CON) or treated with 4 mg l^{-1} IAA (IAA), showing IAA treatment induced displacements of the peaks or changes in absorbance. (C, D) Typical score plots obtained from principal component analysis applied to the cell-wall spectra in the apical region (C) and subapical region (D) for the IAA-treated (IAA) and the control (CON) tubes. Best separation was obtained with the first principal component (PC1) score. (E, F) Difference spectra generated by digital subtraction of CON spectra from IAA spectra of the apical (E) or subapical region (F), showing that the content of proteins and pectin increased while the content of cellulose decreased after IAA treatment.

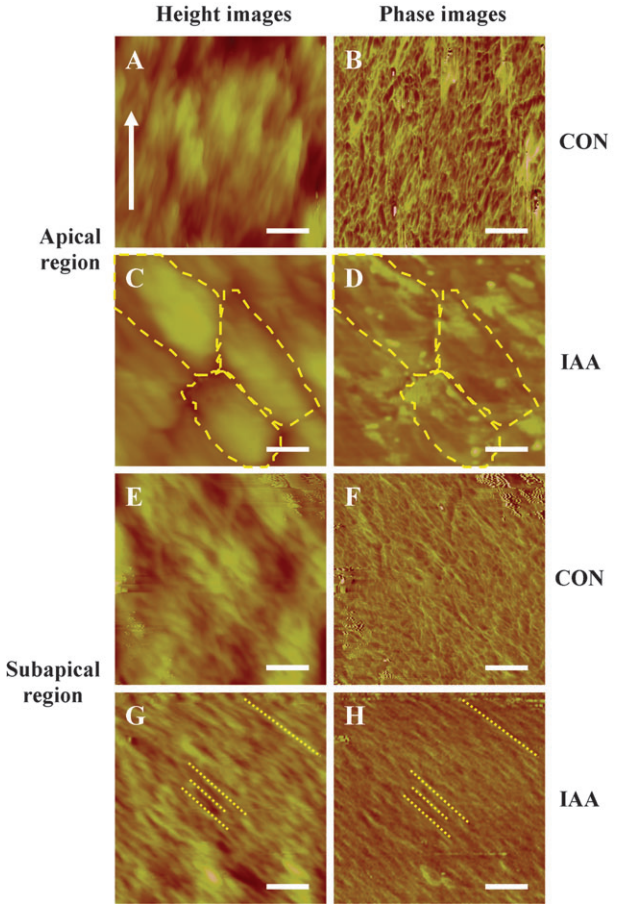

Fig. 8. AFM images of pollen tubes in *Torenia fournieri*. The height images (A, C, E, G) and corresponding phase images (B, D, F, H) in apical region (A–D) and the subapical region (E–H) of control (CON) (A, B, E, F) and IAA-treated pollen tubes (IAA) (C, D, G, H). The growth direction of pollen tubes in all images was upright (as an arrow in A). The block-like structures are outlined with dashes in (C) and (D), and the fibrous structures are indicated with dotted lines in (G) and (H). Bars = 200 nm (A–H).

Table 3. *Quantitative analysis of block-like and fibrous structures in* in vitro *pollen tubes of* Torenia fournieri *based on AFM images*

Values given in the table are means and standard errors of 20 samples measured. The analysis of significant variance was performed between the control group and IAA treatment according to Student's unpaired *t*-test.

Region	Treatment	Structure	Height (nm)[a]	Diameter (nm)[a]
Apex	Control	Block-like	4.4±1.4	27.3±4.0
	IAA	Block-like	9.7±4.0***	72.0±14.3***
Subapex	Control	Block-like	7.8±3.2	52.2±11.8
		Fibrous	3.4±0.9	26.7±3.2
	IAA	Block-like	3.8±0.8***	42.1±8.0***
		Fibrous	2.7±0.7**	28.1±2.9*

[a]* $P > 0.05$ indicates no difference; ** $0.01 < P < 0.05$ indicates distinct difference; *** $P < 0.01$ indicates extreme distinct difference.

1997; Feijo *et al*., 1999). Furthermore, in *L. longiflorum*, fusicoccin activated PM H^+-ATPase and stimulated pollen tube growth, but did not change the cytoplasmic pH (Fricker *et al*., 1997). All these studies showed that, so far, the relationship is unclear between the PM H^+-ATPases, the pH_{cyt} gradients, and the tip H^+ influx, as well as the mechanism of PM H^+-ATPases in pollen tube. Nevertheless, PM H^+-ATPase has been proved to participate in auxin-mediated cell elongation such as in maize coleoptiles and wheat embryo scutellum (Frias *et al*., 1996; Rober-Kleber *et al*., 2003). In the present study, IAA increased the level of PM H^+-ATPases in the pollen tube, presuming that PM H^+-ATPase is involved in IAA-induced pollen tube growth.

IAA stimulates the synthesis of pectin in pollen tubes

Cell growth is intimately linked with cell wall expansion which is generally well co-ordinated with wall polymer synthesis and secretion. Esterified pectin is one of the main components of the wall at the pollen tube tip and is responsible for high elasticity and plasticity of the tube tip (Parre and Geitmann, 2005). Esterified pectin is synthesized within the Golgi complex and then transported to the tube tip through SVs (Bosch and Hepler, 2005). In general, esterified pectin is restricted to the tip region of the pollen tube while acid pectin is found in the shank of pollen tubes and is absent from the apical tube wall (Bosch and Hepler, 2005; Parre and Geitmann, 2005; Röckel *et al*., 2008). However, some independent studies demonstrated the presence of esterified pectin in both the apex and the shank of the pollen tube and the distribution of acid pectin along the entire length of the pollen tube in *Ornithogalum virens* (Stepka *et al*., 2000). In the present study, the distribution pattern of pectins was investigated in detail as pollen tubes grew, and it was found that the distribution of the esterified pectin was a dynamic process, i.e. it was distributed along the entire pollen tube at an early stage of growth and was gradually concentrated at the tube tips as pollen tubes grew (Fig. 5C–F). Also in the present study, immunolabelling and FTIR analysis revealed that esterified pectin was more abundant in IAA-treated tubes than in control tubes (Figs 5, 7). The results agreed with an increase in numbers of SVs in the tube tip and directly demonstrated that IAA could stimulate pectin synthesis and secretion, which might help to enhance the extensibility of the tube tip and stimulate tube growth.

It is widely known that acid pectin originates from the de-esterification of esterified pectin, which is mediated by pectin methylesterases (PMEs) (Parre and Geitmann, 2005; Krichevsky *et al*., 2007). In the present study, IAA induced more acid pectin formation in pollen tubes. PME genes encode isoforms with a different action pattern. The alkaline PME isoforms execute blockwise de-esterification and induce acid pectin to cross-link with Ca^{2+}, resulting in cell wall stiffening. On the other hand, the acidic isoforms execute random de-esterification which results in cell wall loosening (Micheli, 2001). Various PMEs, including

acidic, neutral, and alkaline isoforms, were detected in pollen tubes (Li *et al*., 2002) and the inhibition of PME activity significantly retarded tube growth (Jiang *et al*., 2005). Furthermore, auxin is believed to increase PME activity and stimulate cell wall extension (Micheli, 2001). It was considered that the increased acid pectin in IAA-treated tubes might be attributed to the increased PME activity which may not only control tube growth rate but also tube wall architecture.

CMF orientation is correlated with growth rate and growth direction of pollen tubes

The distribution pattern of cellulose in pollen tubes has been investigated for years without a verdict. For example, CMFs are detected in regions 5–15 μm away from the tube tips of tobacco (Ferguson *et al*., 1998), while they occur close to the tube tip of conifer (Lazzaro *et al*., 2003). In the present study, CW-labelling experiments showed that the cellulose distribution pattern changed temporally and spatially; namely, cellulose was distributed throughout the freshly germinated pollen tubes and was absent from the tube tip as the pollen tube grew long enough (Fig. 6). CW labelling and FTIR analysis also revealed that the relative cellulose density became lower in the pollen tube, especially in the tube tip after IAA treatment (Figs 6, 7; Table 2), which was consistent with the AFM observation that abundant CMFs formed a network in the apical region of slow-growing control tubes (Fig. 8B); however, few CMFs were observed in the IAA-treated tube tip (Fig. 8D). The results indicated a significant correlation between cellulose and pollen tube growth in response to IAA. Lazzaro *et al*. (2003) reported that conifer pollen tubes with more cellulose depositing in the tube tip grew much slower than angiosperm pollen tubes. They speculated that cellulose inserted in the tube tip limited conifer pollen tube expansion. The present observation of accelerated tube growth induced by IAA accompanied by lowered cellulose density in the tube tip, was consistent with this hypothesis. Therefore, it is suggested that the interlaced CMFs in the pollen tube tip of *T. fournieri* lead to loss of the wall's ability to grow and that cellulose is involved in IAA-induced tube growth.

However, no significant difference was found in the total cellulose fluorescence value of pixels falling within the tubes between control and IAA-treated tubes (Table 2), which indicated that cellulose synthesis was not influenced by IAA. A similar result was reported in IAA-induced elongations of *Pellia* setae that the synthesis of other wall polysaccharides, but not cellulose, was enhanced (Thomas *et al*., 1984). Furthermore, inhibitor tests also showed that the synthesis of cellulose is not required for IAA-induced elongation of rice coleoptile segments (Hoson and Masuda, 1992). Thus, it was supposed that cellulose synthesis is also not affected by IAA in pollen tube growth.

Deposition and rearrangement of CMFs within cell-wall matrices is considered to be one of the most critical steps in the regulation of cell shape and expansion direction (Roudier *et al*., 2005). The orientation of CMFs was extensively investigated in diffuse growth cells, such as root cells, and it indicated that CMF orientation was nearly perpendicular to the main axis of cell expansion, especially in rapidly elongating cells (Sugimoto *et al*., 2000; Baskin, 2001). However, in the case of highly polarized tip-growing pollen tubes, little attention was paid to the relationship of the tube shape and growth direction with the organization of CMFs, and knowledge about the orientation of CMFs is scarce. In early reports, CMFs prepared from the extracted pollen tube wall showed a preferential angle of 45° to the longitudinal axes in the shank of petunia and lily pollen tubes, whereas they seemed to be random at the tip of the pollen tube in petunia (Sassen, 1964; Derksen *et al*., 1999). These observations indicated that the mechanism by which CMFs control growth direction may be different between tip growth and diffuse growth to a certain extent. The orientation of CMFs in diffuse growth can be precisely controlled by hormones. In growing tissues of higher plants, auxin induced a shift of CMF arrangement from longitudinal to transverse, which was correlated with promotion of elongation (Shibaoka, 1991). In the present study, AFM images can offer *in situ* information on CMF orientation of the very outer surface of pollen tubes, and showed that CMFs formed random networks in the apical and subapical regions of control tubes (Fig. 8B, F), while CMFs were parallel to each other and presented predominant orientation about 45° to the longitudinal axis of IAA-treated tubes in the subapical region (Fig. 8H). The results suggested that IAA can control the orientation of CMFs in the tip-growing pollen tube. There was a similar phenomenon reported in tobacco mesophyll protoplasts that CMFs changed from a 'random' arrangement into an ordered orientation in the auxin-induced long tubular cells. It indicated that auxin could induce CMF reorientation and determine the axis of cell growth (Vissenberg *et al*., 2000). Moreover, it suggested that a parallel orientation of the newly synthesized CMFs permitted cell growth restricted to one direction (Green, 1980). It was speculated that in IAA-treated tubes the parallel CMFs lead to a predominant growth direction along longitudinal axes of the tubes with narrowed diameter, and that in control tubes, a sinuous CMF network results in multi-direction growth which is concomitant with a wavy shape and a wide diameter pollen tube.

However, in IAA-treated tubes it was still inexplicable that few CMFs were observed in the apical region, while parallel-orientated CMFs occur in the subapical region. Recently, it was reported that microtubes are generally

long and axially orientated in the distal part of the pollen tube and absent in the very tip of *Papaver rhoeas*. It was suggested that microtubes played an important role in controlling the direction of pollen tube growth in the distal part of the tube, but not in the very tube tip (Gossot and Geitmann, 2007). Furthermore, it is well known that microtubes control the deposition of CMFs (Giddings and Staehelin, 1991). Therefore, it was thought that CMFs in the subapical region of the tubes are a crucial factor in regulating the tube growth rate and direction.

Tapping mode AFM is a useful technique to discern the CMF arrangement in situ *in pollen tube walls*

For such samples as pollen tubes, the *in situ* imaging for the region of interest is crucial because of the compositive and configurational difference along the longitudinal axis. Tapping mode AFM is a non-destructive technique for high-resolution surface imaging, with the advantages of easy sample preparation and *in situ* observation (Ding and Himmel, 2006). In the present experiments, the AFM tip was located precisely over the midpoint region of the very apex of the tube tip (apical region) and the subapical regions (~130 μm away from the tube tip) of the 'intact' tube wall and tapping mode AFM was used to observe the orientation of the CMFs *in situ*. From the height images, it can obviously be seen that the IAA-treated apical region was different from that of the control (Fig. 8A, C), indicating that IAA changed the ultrastructure of the tube surfaces. AFM has been used to observe directly the CMFs which were reticulated by the matrix constituents in grapevine suspension cells (Lesniewska *et al*., 2004). It is well known that the difference in elasticity of sample surfaces can be discerned in phase images of tapping mode AFM (Ding and Himmel, 2006) and that pectin has higher elasticity than cellulose (Morris *et al*., 1997). The present phase images showed that there were more filaceous structures in the apical region of the control than in the same region of IAA-treated tubes. As shown in CW-labelling experiments, there was more cellulose in the apical region of the control tube than in the same region

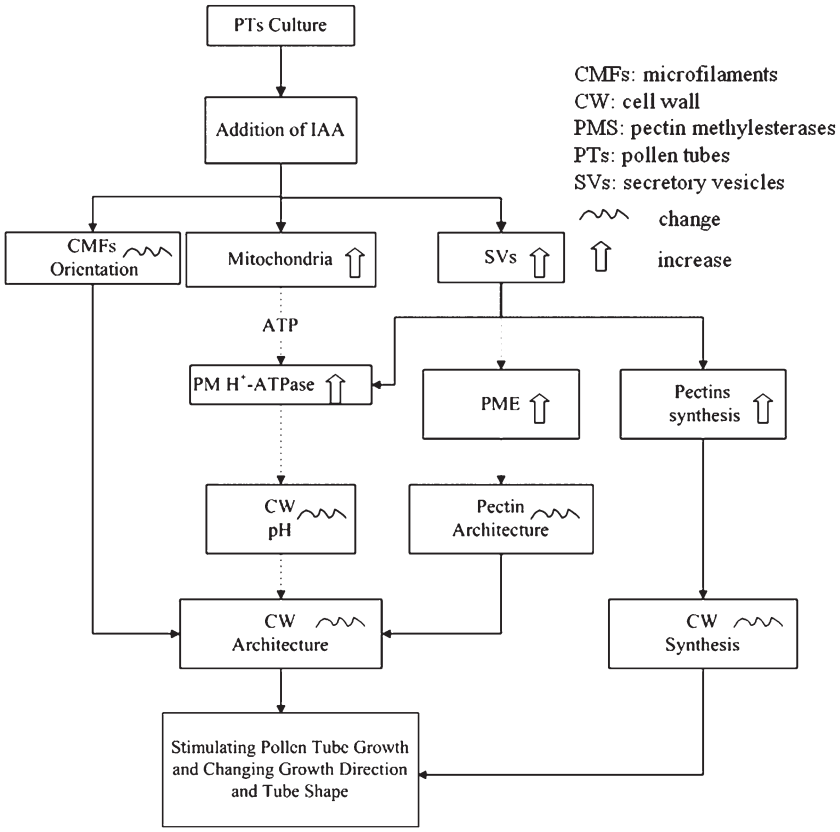

Fig. 9. A hypothetical model for the effects of IAA on pollen tube growth in *Torenia fournieri*. IAA stimulates the amount and activity of mitochondria and the secretion and fusion of SVs in the pollen tube, which transports more cell wall materials (such as pectin) and various enzymes (such as PM H^+-ATPase and PME) into the tube tip. The increase in pectin indicates the enhancement of cell wall synthesis. The increased numbers of mitochondria support more energy (ATP) for various cellular activities such as the execution of PM H^+-ATPase function. The increase in PM H^+-ATPase results in a change in the pH condition of the cell wall, which may lead to the modification of cell wall architecture. The increase of PME activity stimulates the pectin de-esterification process and consequently causes the alteration in pectin architecture. IAA also induces reorientation of cellulose microfibrils in the tube cell wall, which results in modification of the cell wall architecture. Simultaneous cell wall synthesis enhancement and cell wall architecture modification lead to the promotion of pollen tube growth, accompanied by a narrower tube diameter and a straighter tube.

of the IAA-treated tube (Fig. 6G, I). Thus, it can be deduced that the difference in phase images of the apical region may result from the different contents of CMFs. Therefore, the directions of CMFs can be easily discerned in phase images. Tapping mode AFM is a powerful technique for examining the orientation of CMFs *in situ* and analysing the 'intact' pollen tube wall.

Conclusion

In summary, the present investigations clearly confirmed that IAA stimulated the growth of *T. fournieri* pollen tubes by increasing the secretion of SVs and PM H^+-ATPase, and modifying the tube wall composition and structure, especially CMF orientation, which is summarized in Fig. 9. This study highlighted the role of the cell wall, especially CMF orientation, in pollen tube growth and direction.

Acknowledgements

The authors thank Dr JP Knox (Centre for Plant Sciences, University of Leeds, UK) for the generous gifts of the antibodies JIM5 and JIM7, Professor Jinxing Lin (Institute of Botany, Chinese Academy of Sciences, Key Laboratory of Photosynthesis and Molecular Environment Physiology, China) for the generous gift of FM4-64, and Professor Marc Boutry (Unité de Biochimie Physiologique, Institut des Sciences de la Vie, Université Catholique de Louvain-la-Neuve) for the generous gift of the anti-PM-H^+-ATPase antibody. The authors also thank Dr Jun'e Qu (the Analysis and Testing Center, Hubei University, China) for her collaboration in AFM experiments. This work was supported by the National Natural Science Foundation of China (30521004), the Special Doctorial Program Funds of the Ministry of Education of China (20050486015), and the National Natural Science Foundation of China (20621502).

References

Addicott FT. 1943. Pollen germination and pollen tube growth, as influenced by pure growth substances. *Plant Physiology* **18,** 270–279.

Aloni R, Aloni E, Langhans M, Ullrich CI. 2006. Role of auxin in regulating *Arabidopsis* flower development. *Planta* **223,** 315–328.

Barron C, Parker ML, Mills EN, Rouau X, Wilson RH. 2005. FTIR imaging of wheat endosperm cell walls *in situ* reveals compositional and architectural heterogeneity related to grain hardness. *Planta* **220,** 667–677.

Baskin TI. 2001. On the alignment of cellulose microfibrils by cortical microtubules: a review and a model. *Protoplasma* **215,** 150–171.

Bosch M, Hepler PK. 2005. Pectin methylesterases and pectin dynamics in pollen tubes. *The Plant Cell* **17,** 3219–3226.

Chauhan YS, Katiyar SR. 1998. Effects of radiation and growth hormones on pollen germination, pollen tube growth and modulation of radiation responses of *Pinus kesiya Royle ex Gord*. *Cytologia* **63,** 341–348.

Cresti M, Ciampolini F, Mulcahy DLM, Mulcahy G. 1985. Ultrastructure of *Nicotiana alata* pollen, its germination and early tube formation. *American Journal of Botany* **72,** 719–727.

Derksen J, van Amstel ANM, Rutten ALM, Knuiman B, Li YQ, Pierson ES. 1999. Pollen tubes: cellular organization and control of growth. In: Clement C, Pacini E, Audran JC, eds. *Anther and pollen*. Berlin: Springer, 161–174.

Ding SY, Himmel ME. 2006. The maize primary cell wall microfibril: a new model derived from direct visualization. *Journal of Agriculture and Food Chemistry* **54,** 597–606.

Feijo JA, Sainhas J, Hackett GR, Kunkel JG, Hepler PK. 1999. Growing pollen tubes possess a constitutive alkaline band in the clear zone and a growth-dependent acidic tip. *Journal of Cell Biology* **144,** 483–496.

Ferguson C, Teeri TT, Siika-aho M, Read SM, Basic A. 1998. Location of cellulose and callose in pollen tubes and grains of *Nicotiana tabacum*. *Planta* **206,** 452–460.

Frias I, Caldeira MT, Perez-Castineira JR, Navarro-Avino JP, Culianez-Macia FA, Kuppinger O, Stransky H, Pages M, Hager A, Serrano R. 1996. A major isoform of the maize plasma membrane H (+)-ATPase: characterization and induction by auxin in coleoptiles. *The Plant Cell* **8,** 1533–1544.

Fricker MD, White NS, Obermeyer G. 1997. pH gradients are not associated with tip growth in pollen tubes of *Lilium longiflorum*. *Journal of Cell Science* **110,** 1729–1740.

Geitmann A, Parre E. 2004. The local cytomechanical properties of growing pollen tubes correspond to the axial distribution of structural cellular elements. *Sexual Plant Reproduction* **17,** 9–16.

Geitmann A, Steer M. 2006. The architecture and properties of the pollen tube cell wall. In: Malhó R, ed. *The pollen tube*. *Plant Cell Monographs*, Vol. 3. Berlin: Springer Verlag, 177–200.

Giddings TH, Staehelin LA. 1991. Microtubule-mediated control of microfibril deposition: a re-examination of the hypothesis. In: Lloyd CW, ed. *The cytoskeletal basis of plant growth and form*. San Diego, CA: Academic Press, 85–100.

Gossot O, Geitmann A. 2007. Pollen tube growth: coping with mechanical obstacles involves the cytoskeleton. *Planta* **226,** 405–416.

Green PB. 1980. Organogenesis – a biophysical view. *Annual Review of Plant Physiology* **31,** 51–82.

Hepler PK, Vidali L, Cheung AY. 2001. Polarized cell growth in higher plants. *Annual Review of Cell and Developmental Biology* **17,** 159–187.

Higashiyama T, Haruko Kuroiwa H, Kawano S, Kuroiwa T. 1998. Guidance *in vitro* of the pollen tube to the naked embryo sac of *Torenia fournieri*. *The Plant Cell* **10,** 2019–2031.

Hoson T, Masuda Y. 1992. Relationship between polysaccharide synthesis and cell wall loosening in auxin-induced elongation of rice coleoptile segments. *Plant Science* **83,** 149–154.

Jiang LX, Yang SL, Xie LF, Puah CS, Zhang XQ, Yang WC, Sundaresan V, Ye D. 2005. VANGUARD1 encodes a pectin methylesterase that enhances pollen tube growth in the *Arabidopsis* style and transmitting tract. *The Plant Cell* **17,** 584–596.

Jones L, Milne JL, Ashford D, McCann MC, McQueen-Mason SJ. 2005. A conserved functional role of pectic polymers in stomatal guard cells from a range of plant species. *Planta* **221,** 255–264.

Kovaleva L, Zakharova E. 2003. Hormonal status of the pollen-pistil system at the progamic phase of fertilization after compatible and incompatible pollination in *Petunia hybrida* L. *Sexual Plant Reproduction* **16,** 191–196.

Krichevsky A, Kozlovsky SV, Tian GW, Chen MH, Zaltsman A, Vitaly Citovsky V. 2007. How pollen tubes grow. *Developmental Biology* **303,** 405–420.

Lazzaro MD, Donohue JM, Soodavar FM. 2003. Disruption of cellulose synthesis by isoxaben causes tip swelling and disorga-

nizes cortical microtubules in elongating conifer pollen tubes. *Protoplasma* **220,** 201–207.

Lefebvre B, Arango M, Oufattole M, Crouzet J, Purnelle B, Boutry M. 2005. Identification of a *Nicotiana plumbaginifoli*a plasma membrane H (+)-ATPase gene expressed in the pollen tube. *Plant Molecular Biology* **58,** 775–787.

Lesniewska E, Adrian M, Klinguer A, Pugin A. 2004. Cell wall modification in grapevine cells in response to UV stress investigated by atomic force microscopy. *Ultramicroscopy* **100,** 171–178.

Li YQ, Mareck A, Faleri C, Moscatelli A, Liu Q, Cresti M. 2002. Detection and localization of pectin methylesterase isoforms in pollen tubes of *Nicotiana tabacum* L. *Planta* **214,** 734–740.

Maudoux O, Batoko H, Oecking C, Gevaert K, Vandekerckhove J, Boutry M, Morsomme P. 2000. A plant plasma membrane H^+-ATPase expressed in yeast is activated by phosphorylation at its penultimate residue and binding of 14-3-3 regulatory proteins in the absence of fusicoccin. *Journal of Biological Chemistry* **275,** 17762–17770.

Micheli F. 2001. Pectin methylesterases: cell wall enzymes with important roles in plant physiology. *Trends in Plant Science* **6,** 414–419.

Mol R, Filek M, Machackova I, Matthys-Rochon E. 2004. Ethylene synthesis and auxin augmentation in pistil tissues are important for egg cell differentiation after pollination in maize. *Plant and Cell Physiology* **45,** 1396–1405.

Moller IM. 2001. Plant mitochondria and oxidative stress: electron transport, NADPH turnover, and metabolism of reactive oxygen species. *Annual Review of Plant Physiology & Plant Molecular Biology* **52,** 561–591.

Morris VJ, Gunning AP, Kirby AR, Round A, Waldron K, Ng A. 1997. Atomic force microscopy of plant cell walls, plant cell wall polysaccharides and gels. *International Journal of Biological Macromolecules* **21,** 61–66.

Nemhauser JL, Feldman LJ, Zambryski PC. 2000. Auxin and *ETTIN* in *Arabidopsis* gynoecium morphogenesis. *Development* **127,** 3877–3888.

Obermeyer G, Lutzelschwab M, Heumann HG, Weisenseel MH. 1992. Immunolocalization of H^+-ATPases in the plasma membrane of pollen grains and pollen tubes of *Lilium longiflorum*. *Protoplasma* **171,** 55–63.

Parre E, Geitmann A. 2005. Pectin and the role of the physical properties of the cell wall in pollen tube growth of *Solanum chacoense*. *Planta* **220,** 582–592.

Parton RM, Fischer S, Malho R, Papasouliotis O, Jelitto TC, Leonard T, Read ND. 1997. Pronounced cytoplasmic pH gradients are not required for tip growth in plant and fungal cells. *Journal of Cell Science* **110,** 1187–1198.

Parton RM, Fischer-Parton S, Watahiki MK, Trewavas AJ. 2001. Dynamics of the apical vesicle accumulation and the rate of growth are related in individual pollen tubes. *Journal of Cell Science* **114,** 2685–2695.

Pertl H, Himly M, Gehwolf R, Kriechbaumer R, Strasser D, Michalke W, Richter K, Ferreira F, Obermeyer G. 2001. Molecular and physiological characterisation of a 14-3-3 protein from lily pollen grains regulating the activity of the plasma membrane H^+-ATPase during pollen grain germination and tube growth. *Planta* **213,** 132–141.

Raghavan V, Baruah HK. 1956. On factors influencing fruit-set and sterility in arecanut (*Areca catechu* Linn.). II. Germination of pollen grains and growth of pollen tube under the influence of certain auxin, vitamins and trace elements. *Phyton* **7,** 77–82.

Raghavan V, Baruah HK. 1959. Effect of time factor on the stimulation of pollen germination and pollen tube growth by certain auxins, vitamins, and trace elements. *Physiologia Plantarum* **12,** 441–451.

Rayle DL, Cleland RE. 1992. The acid growth theory of auxin-induced cell elongation is alive and well. *Plant Physiology* **99,** 1271–1274.

Rober-Kleber N, Albrechtova JT, Fleig S, Huck N, Michalke W, Wagner E, Speth V, Neuhaus G, Fischer-Iglesias C. 2003. Plasma membrane H^+-ATPase is involved in auxin-mediated cell elongation during wheat embryo development. *Plant Physiology* **131,** 1302–1312.

Röckel N, Wolf S, Kost B, Rausch T, Greiner S. 2008. Elaborate spatial patterning of cell-wall PME and PMEI at the pollen tube tip involves PMEI endocytosis, and reflects the distribution of esterified and de-esterified pectins. *The Plant Journal* **53,** 133–143.

Roudier F, Fernandez AG, Fujita M, Himmelspach R, Borner GHH, Schindelman G, Song S, Baskin TI, Dupree P, Wasteneys GO, Benfey PN. 2005. COBRA, an *Arabidopsis* extracellular glycosyl-phosphatidyl inositol-anchored protein, specifically controls highly anisotropic expansion through its involvement in cellulose microfibril orientation. *The Plant Cell* **17,** 1749–1763.

Sassen MMA. 1964. Fine structure of *Petunia* pollen grain and pollen tube. *Acta Botanica Neerlandica* **13,** 175–181.

Sheng X, Hu Z, Lu H, Wang X, Baluska F, Samaj J, Lin J. 2006. Roles of the ubiquitin/proteasome pathway in pollen tube growth with emphasis on MG132-induced alterations in ultrastructure, cytoskeleton, and cell wall components. *Plant Physiology* **141,** 1578–1590.

Shibaoka H. 1991. Microtubules and the regulation of cell morphogenesis by plant hormones. In: Lloyd CW, ed. *The cytoskeletal basis of plant growth and form.* London: Academic Press, 159–168.

Stepka M, Ciampolimi F, Cresti M. 2000. Localization of pectins in the pollen tube wall of *Ornithogalum virens*: does the pattern of pectin distribution depend on the growth rate of the pollen tube? *Planta* **210,** 630–635.

Sugimoto K, Williamson RE, Wasteneys GO. 2000. New techniques enable comparative analysis of microtubule orientation, wall texture and growth rate in intact roots of *Arabidopsis*. *Plant Physiology* **124,** 1493–1506.

Synytsya A, Copikova J, Matejka P, Machovic V. 2003. Fourier transform raman and infrared spectroscopy of pectins. *Carbohydrate Polymer* **54,** 97–106.

Thomas RJ, Behringer FJ, Lombard CS, Sparkowski JJ. 1984. Effects of auxin on wall polysaccharide composition and enzyme activity during extension-growth of *Pellia* (Bryophyta). *Physiologia Plantarum* **60,** 502–506.

Toole GA, Kakurakova M, Smith AC, Waldron KW, Wilson RH. 2004. FT-IR study of the *Chara corallina* cell wall under deformation. *Carbohydrate Research* **339,** 629–635.

Vissenberg K, Quelo AH, Van Gestel K, Olyslaegers G, Verbelen JP. 2000. From hormone signal, via the cytoskeleton, to cell growth in single cells of tobacco. *Cell Biology International* **24,** 343–349.

Wu JZ, Qin Y, Zhao J. 2008. Pollen tube growth is affected by exogenous hormones and correlated with hormone changes in styles before and after pollination in *Torenia fournieri* L. *Plant Growth Regulation* DOI: 10.1007/s10725-008-9268-5.

Zhang LY, Fang KF, Lin JX. 2005. Heterotrimeric G protein α-subunit is localized in the plasma membrane of *Pinus bungeana* pollen tubes. *Plant Science* **169,** 1066–1073.

Zhao J, Yu FL, Liang SP, Zhou C, Yang HY. 2002. Changes of calcium distribution in egg cells, zygotes and two-celled proembryos of rice (*Oryza sativa* L.). *Sexual Plant Reproduction* **14,** 331–337.